Parameter Estimation of a Mathematical Model for Lower-Limb Exoskeletons with Paralysed Humans

Norazam Aliman[1, a)], Adi Izhar Che Ani[2, b)], Hazman Abu Hassan[3, c)]

[1]*Department of Mechanical Engineering, Politeknik Sultan Azlan Shah, Behrang Stesen, 35950 Behrang, Perak, Malaysia*
[2]*Electrical Engineering Studies, Universiti Teknologi MARA Cawangan Pulau Pinang, Kampus Permatang Pauh*
13500 Pulau Pinang, Malaysia
[3]*Department of Mechanical Engineering, Politeknik Sultan Azlan Shah, Behrang Stesen, 35950 Behrang, Perak, Malaysia*

[a)]Corresponding author: norazam_aliman@psas.edu.my
[b)]adiizhar@uitm.edu.my
[c)]hazman.hassan@psas.edu.my

Received 1 October 2025, Accepted 28 October 2025, Available Online 30 November 2025

Abstract. The development of dynamic models for rehabilitation lower-limb exoskeletons (RLLEs) integrated with human interaction (RLLE–Patient) has been proposed by numerous researchers. However, due to the nonlinear characteristics of these systems, accurate modelling remains a critical challenge, requiring approaches that are both simple and effective in representing actual scenarios. Therefore, this paper proposes a method for developing and controlling an RLLE-Patient model that accurately replicates real rehabilitation conditions. The RLLE and human models are initially designed in CATIA and transferred to ADAMS, while the direct current motors driving the RLLE joints are modelled in MATLAB Simulink, with motor parameters identified using a parameter estimation tool. A co-simulation between ADAMS and MATLAB is employed to create a comprehensive RLLE-Patient model. Additionally, a virtual Proportional-Integral-Derivative (PID) controller is developed to regulate the dynamic motion of the RLLE, and its performance is evaluated through simulations. The results demonstrate that this method effectively facilitates the design, tuning, evaluation, and improvement of the PID controller's performance in RLLE applications. Further optimization of the control system can be achieved by integrating the dynamic characteristics into the RLLE-Patient model.

Keywords: *lower limb exoskeleton; modelling; parameter estimation; Matlab-ADAMS, co-simulation*

INTRODUCTION

Most patient with spinal cord injuries typically rely on wheelchairs for daily mobility. However, rehabilitation lower-limb exoskeletons (RLLEs) provide a practical alternative, aiding both permanent and temporary patients in rehabilitation and the recovery of movement (Aliman et al., 2024). An RLLE is a mechanical device integrated with electronic components such as power supply, sensors, actuators, and control system. In the early stages of control system development, modeling simulations are commonly used. To ensure the simulation accurately represents real-world conditions, the model must closely mimic the actual scenario. In developing RLLE-Patient modeling, a significant challenge lies in addressing their nonlinear behavior. These nonlinearities arise from both structured and unstructured uncertainties, which add complexity to the modeling system. Structured uncertainties refer to time-varying RLLE characteristics, such as changes in a subject's properties like height and mass. Unstructured uncertainties include factors such as sensor noise, operational speed, external disturbances, and motion friction.

The RLLE models have been extensively explored and developed in the literature. A fundamental approach to modeling involves the use of Newton–Euler equations, as demonstrated by Amiri & Ramli, 2024. This method

enables torque control through a virtual approach but only considers the mechanical structure of the RLLE in mathematical terms. Velandia et al., 2016 introduced a model that integrates the motor and exoskeleton structure using mathematical equations. Similarly, Guo et al., 2015 proposed a model that combines the human limb, mechanical structure and the actuator. This combination model is represented in a mathematical equation; however, it does not consider the interaction between wearer and mechanical RLLE modeling during actual operation.

In another model, Velandia et al., 2017 introduced a mathematical model of the RLLE that incorporates variables such as body mass and height. However, this model does not fully represent the actual RLLE due to the complexity of combining two distinct systems, those of the human and the exoskeleton. Environmental interactions, such as ground reaction forces, are also difficult to incorporate into mathematical equations. Another approach to the virtual RLLE model was developed by Aliman et al. (2021) and Soleimani Amiri et al. (2020). This method enables the creation of a simulation that virtually integrates the exoskeleton model; however, ground reaction forces are not considered in the simulation.

Therefore, this paper proposes a model of the RLLE-Patient system that considers the nonlinear characteristics and closely reflects real walking conditions. To achieve this, the Hanavan, 1966 human model is adapted for RLLE modeling, while DC motor modeling is applied to the RLLE joints to represent the actual situations. This approach is discussed in next section. The results and discussion are provided in the last section.

METHODOLOGY

The development of RLLE-Patient modelling composed of the DC motor, RLLE structure, patient modelling, supporter and ground. The architecture of RLLE-Human modelling is shown in Figure 1(a) while the RLLE device with patient shown in Figure 1(b). The development of the modeling of each component is provided below.

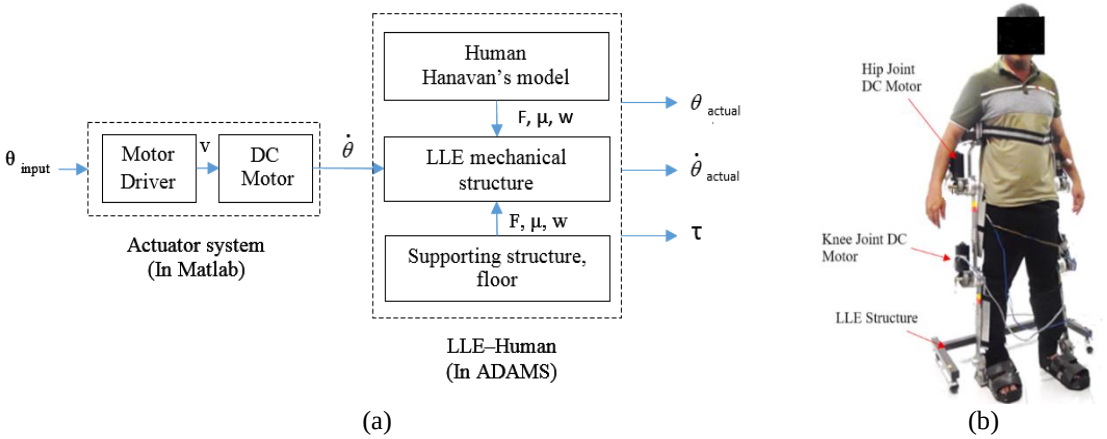

FIGURE 1. (a) Architecture of the RLLE-Patient modelling (b) Actual situation

Actuator modelling

DC motor is used to drive the RLLE joint on both hip and knee which serves to demonstrate the work principle of kinetic energy. Based on the schematic diagram of DC motor shown in Figure 2, the modelling considering the motor and gear ratio n. Thus, the transfer function of input voltage Va(s), to angular velocity, ω(s) is:

$$\frac{\omega(s)}{V_a(s)} = \frac{K_t \times 1/n}{L_a J_m s^2 + (R_a J_m + L_a b_m)s + (R_a b_m + K_b K_t)} \quad (1)$$

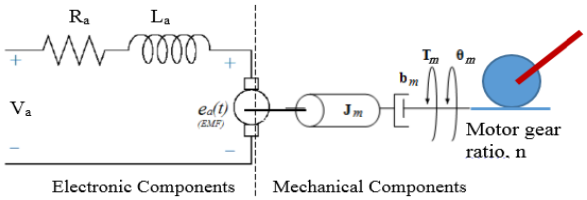

FIGURE 2. Schematic diagram of DC motor

The parameters presented in Equation (1) need to be identified. To facilitate this, the MATLAB Simulink Parameter Estimation tool is employed. The identification process is structured into four phases: experimental setup, data collection, preliminary parameter estimation and model validation. The experimental setup is designed according to the schematic diagram illustrated in Figure 3. The system integrates both hardware and software components, utilizing a pseudo-random binary sequence (PRBS) generator to provide the input signal, (Va) to the motor. The output signals include the angular velocity of the DC motor (ω) and the armature current (ia).

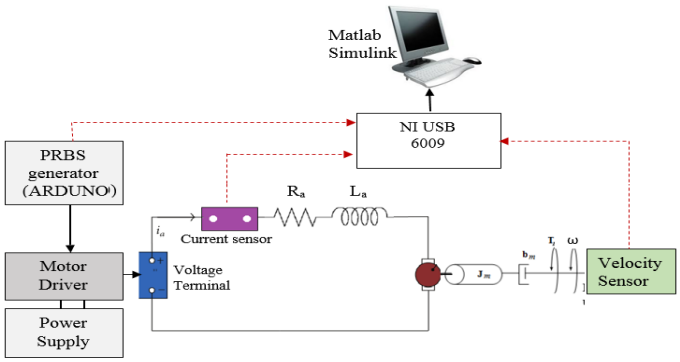

FIGURE 3. Hardware setup for DC motor parameter estimation.

A five-bit PRBS generator was developed using Arduino block sets in MATLAB Simulink, as depicted in Figure 4. The PRBS generator model was subsequently deployed to the Arduino board. To drive the motor, an MD30C motor driver was utilized, capable of handling up to 30 A of current and powered by a 24 V supply. The DC motor speeds were measured by an encoder, thus the PWM on encoder output was converted to angular velocity in analog signal by electronic circuit. The motor current was measured using an ACS756 current sensor. During the experiment, three signals i.e. the PRBS input, motor angular velocity and motor current were simultaneously measured and recorded in the MATLAB workspace. The NI USB 6009 data acquisition system was employed to read and record all signals on the computer. The Matlab Simulink for signal acquisition and recording using the NI USB 6009 Simulink is illustrated in Figure 5.

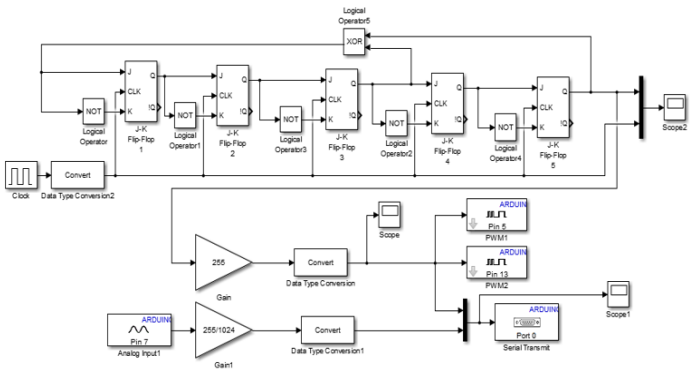

FIGURE 4. PRBS generator in Matlab Simulink

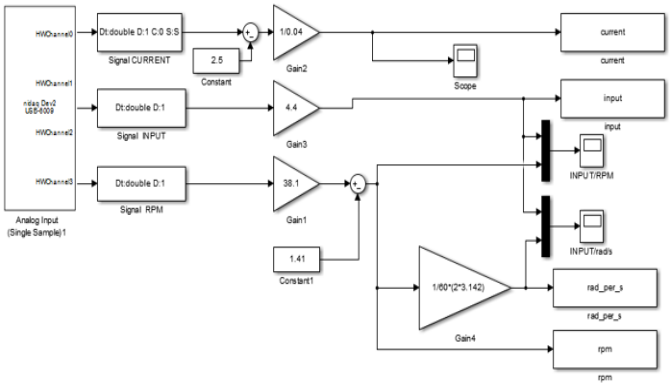

FIGURE 5. NI-USB 6009 Matlab Simulink for data recording in Matlab

In Stage 2, experimental data were collected and initial estimates of the model parameters were obtained. Referring to Equation (1), the parameters requiring identification include L_a, J_m, R_a, B_m, K_b, and K_t, as none of these values were provided by the manufacturer. The voltage input (V_a,), angular velocity (ω) of DC motor shaft, and motor current (i_a) were recorded by an experimental method with 30 s duration, while the armature resistance, R_a and inductor, L_a can be initially estimated using experimental and mathematical calculation. The initial values of R_a and L_a can be determined by mechanically locking the DC motor shaft, thereby setting $\omega(t)=0\omega$ rad/s. Therefore, equation of DC motor becomes:

$$V_a(t) = R_a i_a(t) + L_a \frac{di_a(t)}{dt} \tag{2}$$

With an equation (2), the transfer function is:

$$G(s) = \frac{I_a(s)}{V_a(s)} = \frac{1}{Ls + R} \tag{3}$$

According to equation (3), the gain (steady state output per input) and time constant are $K = 1/R$ and $\tau = L/R$, respectively. With the DC motor rotor locked, and the input voltage $V_a(t)$ = 5V, the current response, ia(t) were obtained. Therefore, the value of K and L for four DC motor were identified based on current response. The values of ω, i_a, R_a, and L_a were read and record by implementing the Simulink model in MATLAB as shown in Figure 5.

Next, in the step 3, the previously identified parameter values were used to estimate the remaining DC motor parameters through the Parameter Estimation Toolbox in MATLAB Simulink. The parameters J_m, B_m, K_b, and K_t were determined by minimizing the total cost function. In step 4, the transfer function model from Equation (1), along with the identified parameters, was validated by comparing the model's response with the actual speed measured during real-time experiments. The pulse generator signal with amplitude of 24 V and period of 20 s is used as input to the estimation model and actual model.

RLLE modelling with patient

The developed RLLE shown in Figure 6(a), consists of eight segments: the RLLE supporter, left and right feet, shanks, thighs, and the waist. The structure features 1 degree of freedom (DOF) at each hip, knee, and ankle joint, allowing rotation in the sagittal plane, as well as 1 DOF at the waist. The RLLE supporter enables vertical motion during walking, while movement in other planes is restricted. The RLLE supporter has been developed to support and maintain the position of RLLE and wearer's load during walking.

The human model is developed based on the Hanavan model, which represents the body using fifteen limb segments. As illustrated in Figure 6(b), the model includes 15 human limbs incorporating anthropometric characteristics (Aliman et al., 2019). Eight joints, including those connecting the upper and lower body, shoulders, elbows, wrists, and neck, are modeled as fixed joints. The remaining six joints in the limb, i.e. hips, knees and

ankles are modeled using spring elements positioned at the center of each joint to simulate joint flexibility and dynamic response.

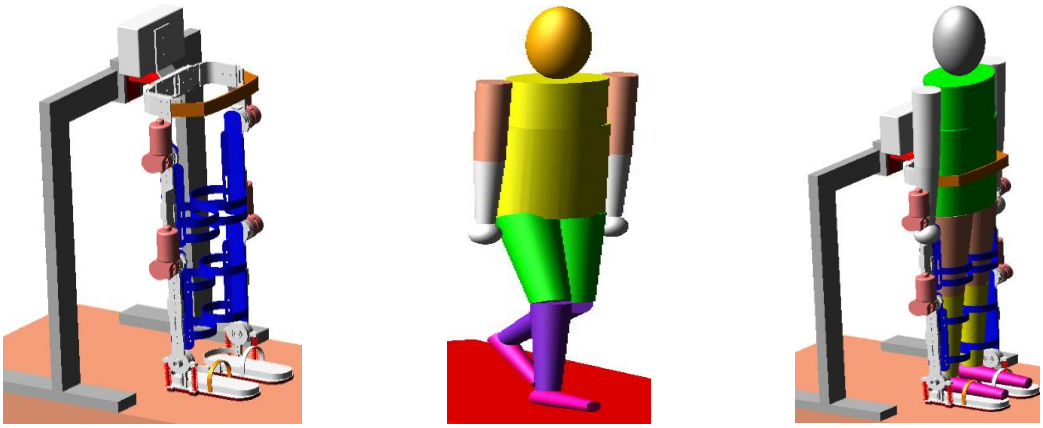

(a) (b) (c)

FIGURE 6. The model in ADAMS a) RLLE structure modelling b) Human modelling. c) RLLE-human modelling

The RLLE-Human model illustrated in Figure 6(c), consists of thirty-six moving parts, including the floor. A total of ten revolute joints are included, located at the shoulders and elbows of the wearer, as well as at the ankles, knees, and hips of the RLLE structure. Seven translational joints are incorporated at the interface between the human waist and RLLE, between each shank and the RLLE, each thigh and the RLLE, between the supporter structure and floor, and between the RLLE and supporter to allow vertical movement during walking. In total, the RLLE-Human model has nine DOF, with one DOF at each hip, knee and ankle joint, one between the supporter and the floor which is constrained in one direction, and one between the waist of RLLE and supporter , which facilitates vertical movement during walking.

The co-simulation was conducted between ADAMS and MATLAB Simulink; therefore, the RLLE Human model developed in ADAMS was exported to MATLAB. As shown in Figure 7, the RLLE-Human subsystem from ADAMS includes four input signals, representing the angular trajectories of the knees and hips, and eight output signals, which correspond to the torque and angular positions of the knee and hip joints.

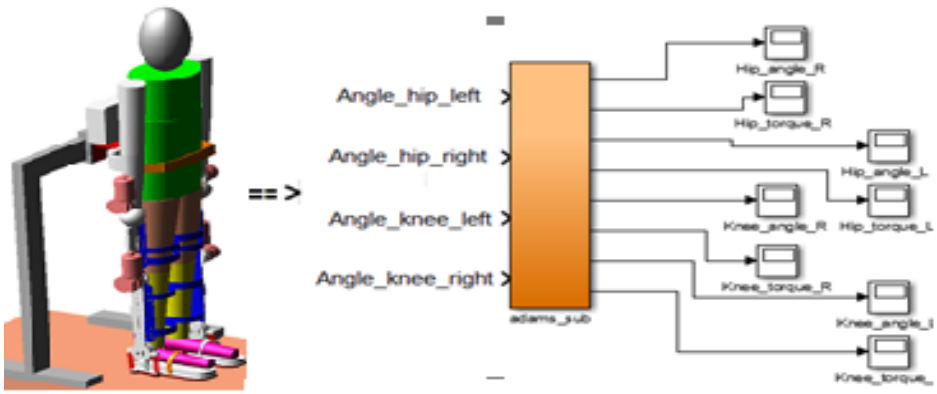

FIGURE 7. RLLE-Human represented by ADAMS sub system in Matlab

Controller development

The control of the DC motors at the RLLE hips and knees is intended to track the RLLE joint movements and follow the input gait trajectory. This is achieved through co-simulation between ADAMS and MATLAB. Since the reference trajectory angles and tracking errors differ for each hip and knee, the PID controller are designed independently for each joint and the controller parameter for both hip and knee are tuned manually until the RLLE

joint angle approaching to zero error. Figure 8 presents the control architecture of the RLLE Human model implemented in the simulation.

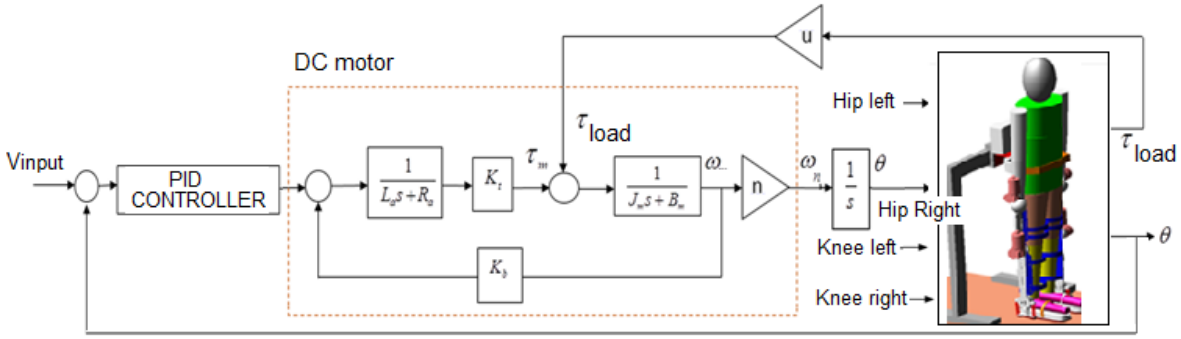

FIGURE 8. Control architecture of RLLE-Human by simulation

RESULT AND DISCUSSION

This The initial values of R_a and L_a were obtained by mechanically locking the DC motor shaft, thereby setting the angular velocity $\omega(t)=0$ rad/s. The identified parameters for R_a and L_a are shown in Table 1. The remaining parameter values for the DC motors at the hip and knee joints, obtained using the Parameter Estimation Toolbox in MATLAB Simulink, are presented in Table 2. Therefore, the response of actual DC motor on each RLLE joint with PRBS input signal is illustrated in Figure 9.

TABLE 1. The identified data for R_a and L_a

DC Motor Parameter	Hip left	Hip right	Knee left	Knee right
Input voltage	5	5	5	5
Steady state current (i_a)	4.9	5.2	4.8	5.0
Resistance (R_a)	1.03	0.962	0.042	1.000
Inductance (L_a)	0.0196	0.0106	0.0073	0.005

TABLE 2. The DC motor parameter of hips and knees

DC Motor Parameter	Hip left	Hip right	Knee left	Knee right
Back emf constant (Kb)	0.18454	0.18516	0.18494	0.18569
Torque constant (Kt)	1.865	1.865	1.953	1.953
Friction coefficient (Bm)	0.0275	0.0268	0.0259	0.0258
Motor inertia (Jm)	0.0293	0.0293	0.0314	0.0318

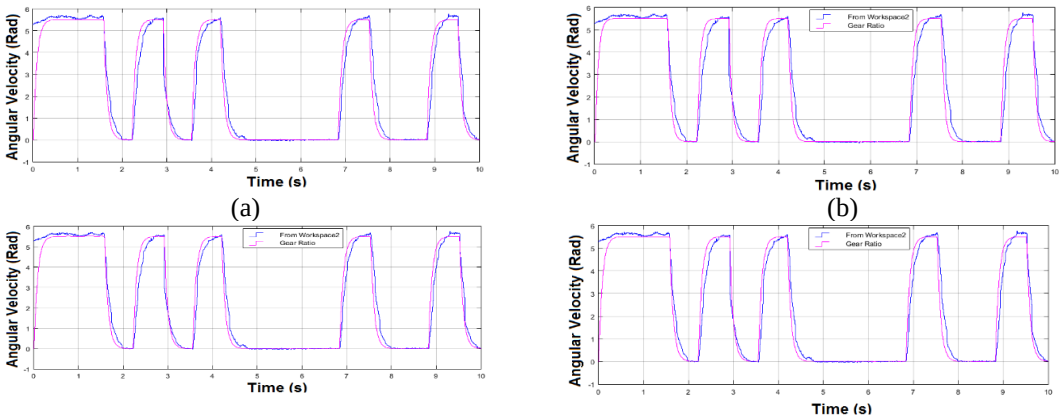

(c) (d)

FIGURE 9. PRBS input response of actual DC motor: a) Hip left b) Knee left c) Hip right d) knee right.

Figure 10 illustrates the output response of the RLLE joint when subjected to the walking trajectory as input, under the PID controller. The DC motor response is evaluated against the reference input signal to assess tracking performance. The simulation results for the hip and knee joints demonstrate the effectiveness of the PID controller in replicating desired joint motion under walking conditions. Figure 11 presents the corresponding torque output generated by the DC motors. The results indicate that the RLLE joint angles successfully follow the reference input with a fast initial response, although the error diminishes gradually over time.

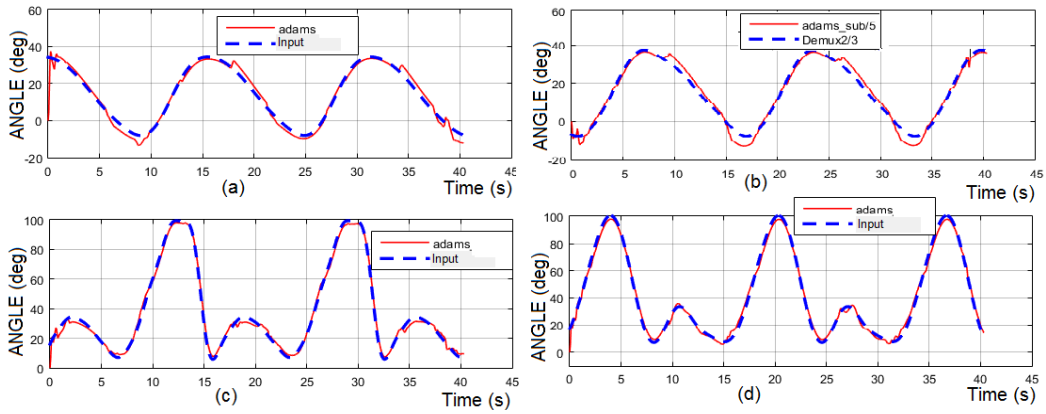

FIGURE 10. Tracking result on: (a) hip left (b) hip right (c) knee left (d) knee right

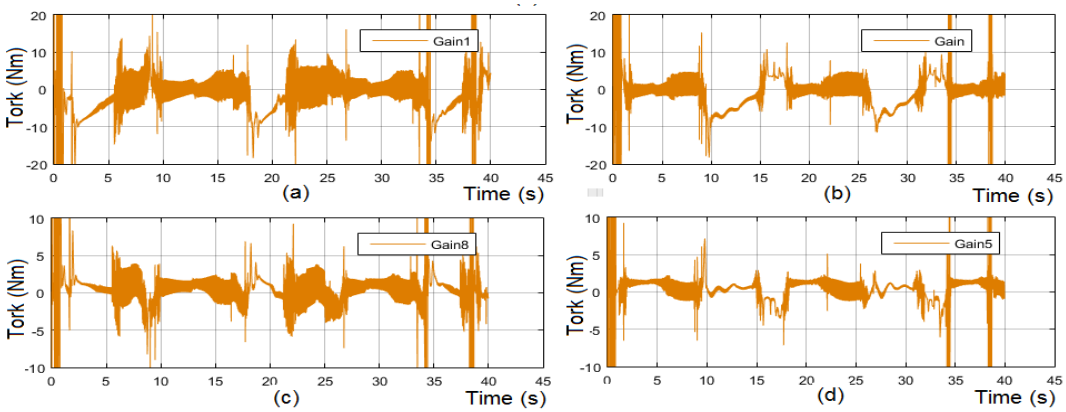

FIGURE 11. Simulation result, torque on: (a) hip left (b) hip right (c) knee left (d) knee right

CONCLUSION

In this study, the design and modelling of the RLLE-Patient system were developed. The dynamic control of the RLLE-Human model was implemented using a PID controller. Simulation was carried out through the co-simulation of ADAMS and MATLAB. This approach simplifies the development of dynamic models, making them easier to implement and closer to real-world device behaviour. The results indicate that the selected DC motor characteristics are appropriate, as the torque output aligns well with the load conditions at the RLLE joints. This method is effective for designing and simulating control systems that emulate human motion. The co-simulation of ADAMS and MATLAB enables accurate evaluation of control performance without the need for physical hardware. For future work, the actual RLLE device will be fabricated, and the controller will be tested on the physical system.

ACKNOWLEDGMENTS

The authors would like to thank all members of the Mechanical Engineering Department at Politeknik Sultan Azlan Shah for their valuable input and strong cooperation throughout this work. This research was supported by the Center for Autonomous Vehicles Technology (CAVTech), Politeknik Sultan Azlan Shah.

REFERENCES

Aliman, N., Ramli, R., & Amiri, M. S. (2024). Actuators and transmission mechanisms in rehabilitation lower limb exoskeletons: a review. Biomedical Engineering / Biomedizinische Technik, 1–19.

Aliman, N., Ramli, R., & Haris, S. M. (2019). Design of locomotive lower limb exoskeleton with Malaysian anthropometric characteristics. International Journal of Mechanical Engineering and Robotics Research, 8(2), 304–309.

Aliman, N., Ramli, R., & Haris, S. M. (2021). Hybrid Design of Model Reference Adaptive Controller and PID Controller for Lower Limb Exoskeleton Application (pp. 539–553).

Amiri, M. S., & Ramli, R. (2024). Admittance swarm-based adaptive controller for lower limb exoskeleton with gait trajectory shaping. Journal of King Saud University - Computer and Information Sciences, 36(1), 101900.

Guo, Q., Li, S., & Jiang, D. (2015). A Lower Extremity Exoskeleton: Human-Machine Coupled Modeling, Robust Control Design, Simulation, and Overload-Carrying Experiment. Mathematical Problems in Engineering, 2015. https://doi.org/10.1155/2015/905761

Hanavan, E. P. (1966). A personalized mathematical model of the human body. Journal of Spacecraft and Rockets, 3(3), 446–448.

Soleimani Amiri, M., Ramli, R., Ibrahim, M. F., Abd Wahab, D., & Aliman, N. (2020). Adaptive Particle Swarm Optimization of PID Gain Tuning for Lower-Limb Human Exoskeleton in Virtual Environment. Mathematics, 8(11), 2040.

Velandia, C. C., Tibaduiza, D. A., & Vejar, M. A. (2017). Proposal of novel model for a 2 DOF exoskeleton for lower-limb rehabilitation. Robotics, 6(3).

Velandia, C., Celedon, H., Tibaduiza, D. A., Torres-Pinzon, C., & Vitola, J. (2016). Design and control of an exoskeleton in rehabilitation tasks for lower limb. 2016 XXI Symposium on Signal Processing, Images and Artificial Vision (STSIVA), 1–6.

Velandia, C., Tibaduiza, D., & Vejar, M. (2017). Proposal of Novel Model for a 2 DOF Exoskeleton for Lower-Limb Rehabilitation. Robotics, 6(3), 20.